Substrate conformational transitions in the active site of chorismate mutase: Their role in the catalytic mechanism

Hong Guo*, Qiang Cui*, William N. Lipscomb*, and Martin Karplus*†‡

*Department of Chemistry and Chemical Biology, Harvard University, 12 Oxford Street, Cambridge, MA 02138; and †Laboratoire de Chimie Biophysique, Institut Le Bel, Université Louis Pasteur, 67000 Strasbourg, France

Contributed by William N. Lipscomb, May 10, 2001

Chorismate mutase acts at the first branch-point of aromatic amino acid biosynthesis and catalyzes the conversion of chorismate to prephenate. The results of molecular dynamics simulations of the substrate in solution and in the active site of chorismate mutase are reported. Two nonreactive conformers of chorismate are found to be more stable than the reactive pseudodiaxial chair conformer in solution. It is shown by QM/MM molecular dynamics simulations, which take into account the motions of the enzyme, that when these inactive conformers are bound to the active site, they are rapidly converted to the reactive chair conformer. This result suggests that one contribution of the enzyme is to bind the more prevalent nonreactive conformers and transform them into the active form in a step before the chemical reaction. The motion of the reactive chair conformer in the active site calculated by using the QM/MM potential generates transient structures that are closer to the transition state than is the stable CHAIR conformer.

Chorismate occupies a central position in the biosynthesis of aromatic amino acids in microorganisms and plants. The isomerization of chorismate to prephenate, the first committed step in the synthesis of tyrosine and phenylalanine (Fig. 1), is formally a Claisen rearrangement and is catalyzed by chorismate mutase (CM) (chorismatepyruvate mutase, EC 5.4.99.5) with a rate enhancement of 2×10^6. The biological importance of this conversion and the synthetic value of the Claisen rearrangement have led to extensive experimental (1–23) and theoretical (24–33) investigations. In particular, the crystal structures of *Bacillus subtilis*, *Escherichia coli* (P-protein), and *Saccharomyces cerevisiae* (yeast) CMs complexed with a transition-state analog (TSA) inhibitor (4) are available (8–11), as well as that of a less active catalytic antibody 1F7 (12). Extensive electrostatic and hydrogen-bonding interactions between the TSA and these enzymes (11) have been examined by site-directed mutagenesis studies (13–17). Nevertheless, many questions remain concerning the details of catalytic processes, including substrate selection, rate enhancement, and roles of active site residues.

Knowles and coworkers demonstrated that the rearrangement of chorismate to prephenate proceeds through a "chair-like" transition state for the atoms of the [3,3]-pericyclic region (Fig. 1), both in solution and in the enzyme-catalyzed reaction (18–19). The bond breaking and making process is presumed to start from a pseudodiaxial (chair) conformer (CHAIR in Fig. 2) that is capable of reaching the transition state directly. One way for CM to speed up the reaction is, therefore, to bind this chair conformer preferentially from solution and to catalyze its chemical transformation at the active site (20). Many discussions of CM catalysis have been based on this mechanism (21, 25, 28–29, 32). However, quantum mechanical calculations (24–25, 27–28, 31) have either failed to identify this reactive conformer in the gas phase or in solution or have found that it is much less stable than some other conformers. For instance, the structure of the "chair-like" transition state was determined by Wiest and Houk (24) from *ab initio* and density functional calculations, but no energy minimum for CHAIR was located in their investigation.

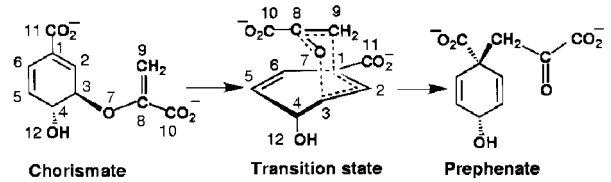

Fig. 1. The Claisen rearrangement of chorismate to prephenate via the proposed "chair-like" transition state where the atoms involved in the [3, 3]-pericyclic reaction are arranged in a chair configuration.

Instead, they obtained a nonreactive extended pseudodiaxial conformer that was used later by Carlson and Jorgensen (27) to study the conformational equilibrium of chorismate in solution. The CHAIR conformer determined by Martí *et al.* (31) from the MP2/6–31G* calculations is 16 kcal/mol less stable than the lowest energy conformer ($DIEQ_2$ in Fig. 2) in the gas phase. Moreover, in a recent transferred nuclear Overhauser effect study of chorismate in solution (23), the CHAIR conformer was not detected. Thus, an alternative to the proposed preferential binding of the CHAIR conformation by the enzyme appears to be required. One possibility is that the enzyme is able to bind the more abundant conformers and convert them to CHAIR in the active site (1, 21–23). In the present paper, this alternative is explored, and the focus is on the dynamics of the substrate conformational transitions in the active site of yeast CM (11). A recently developed potential energy function (34) based on a semiempirical implementation of density functional theory (35) is used. This allows quantum-mechanical/molecular mechanical (QM/MM) molecular dynamics simulations of the substrate in the active site.

Methods

The quantum mechanical calculations for the chorismate substrate conformers in the absence of the enzyme were performed by using the GAUSSIAN98 program (36) with the density functional B3LYP/6–31G* method; the PCM method formulation (37) as implemented in GAUSSIAN98 was used to estimate the effect of aqueous solvation on the energy of the gas-phase conformers. A fast semiempirical density functional approach [self-consistent charge density functional tight-binding (SCC-DFTB) method] (35), recently implemented in the CHARMM

Abbreviations: CM, chorismate mutase; YCM, yeast CM; TSA, transition-state analogue; CHAIR, chair pseudodiaxial conformer; DIAX, a pseudodiaxial conformer; $DIEQ_1$, a pseudodiequatorial conformer; $DIEQ_2$, the lowest energy conformation of chorismate in the gas phase; ex-DIAX, an extended pseudodiaxial conformer; SCC-DFTB, the self-consistent charge density functional tight-binding method; QM/MM, quantum-mechanical/molecular mechanical.

‡To whom reprint requests should be addressed. E-mail: marci@tammy.harvard.edu.

The publication costs of this article were defrayed in part by page charge payment. This article must therefore be hereby marked "*advertisement*" in accordance with 18 U.S.C. §1734 solely to indicate this fact.

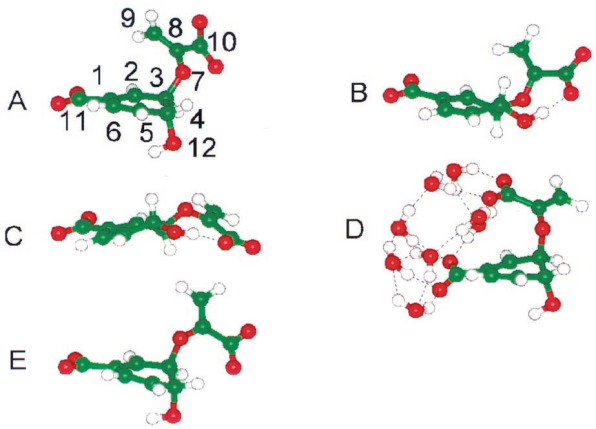

Fig. 2. The gas-phase structures of CHAIR, $DIEQ_1$, $DIEQ_2$, DIAX, and ex-DIAX obtained from geometry optimization at the B3LYP/6–31G* or HF/6–31G* level (see Table 1); the structures obtained from the semiempirical density functional method (SCC–DFTB) are similar (see Table 1). DIAX was also obtained from solution simulations by using CHAIR as the initial conformation. The values of the structural parameters obtained from the solution simulations are close to those from the HF/6–31G* calculations with bridging water molecules (see Table 1). (*A*) CHAIR; (*B*) $DIEQ_1$; (*C*) $DIEQ_2$; (*D*) DIAX; (*E*) ex-DIAX.

program (34), was used for calculations on the same conformers and for comparison with the B3LYP/6–31G* results. Because the values for the stable conformers of chorismate from the two approaches were similar (see *Results*), the SCC-DFTB method was used for QM/MM molecular dynamics simulations in solution and in the enzyme active site; SCC-DFTB calculations are several thousand times faster than those with B3LYP/6–31G*. The chorismate substrate was treated by QM and the rest of the system (explicit aqueous solvent or the enzyme active site) by MM. The quantum mechanical description of the substrate is advantageous because it does not require specific MM parameters to be determined and provides a more realistic treatment of the fluctuations of the covalent bond distances that cleave or form during the reaction (here the ether bond that is broken and the C_1—C_9 bond that is formed during the Claisen rearrangement).The QM/MM molecular dynamics simulations were performed by using the CHARMM program (38); the all-hydrogen potential function (PARAM22) (39) was used for MM atoms. A modified TIP3P water model (40, 41) was used for the solvent. The stochastic boundary molecular dynamics method (42) was used for the QM/MM calculations in the enzyme and in solution.

The initial coordinates for the simulations were obtained from the crystal structure of yeast CM (Protein Data Bank ID code 3csm) in the wild-type "super R" state, which has the TSA plus Trp (ITRP in ref. 11) bound to the active and regulatory sites, respectively. For the simulations, the inhibitor was replaced by the substrate in the various conformations that were examined. In addition to the reactive CHAIR conformer, $DIEQ_1$ and DIAX (see Fig. 2) were studied, because they seemed most likely to be able to change to CHAIR in the active site and were relatively stable in solution; other conformations (e.g., $DIEQ_2$) would have required more complicated motions. Solution simulations were done with and without two unconstrained guanidinium cations. The effects of the latter were examined to mimic the large positive counterions [bis(tetra-*n*-butylammonium)] present in the solution studies of Copley and Knowles (22).

Details of the methods, including the placement of the various conformers in the active site, are published as supplemental data on the PNAS web site (www.pnas.org).

Results

Substrate Conformations from Quantum Mechanical Calculations and from Solution Simulations. To select a set of conformers for introduction into the enzyme active site, gas-phase density functional calculations were made with and without PCM solvation correction and solution QM/MM simulations; the former served also to test the semiempirical SCC-DFTB method. The optimized structures for some of the chorismate conformers (CHAIR, $DIEQ_1$, $DIEQ_2$, and ex-DIAX) from gas-phase calculations are shown in Fig. 2, and their relative stabilities and structural parameters are listed in Table 1. Previous QM calculations (24–25, 27–28, 31) and the present results show that $DIEQ_2$ is the lowest energy conformer in the gas phase and in solution, including PCM solvation correction. Consistent with previous studies (24–25, 27–28, 31), $DIEQ_1$ and $DIEQ_2$ are found to be considerably more stable than CHAIR. Both $DIEQ_1$ and $DIEQ_2$ are stabilized by a strong hydrogen bond between the side-chain carboxylate and the ring OH of C_4 (31). The energy difference ($\Delta E + \Delta\Delta G_{solv}$) between CHAIR and $DIEQ_2$ ($DIEQ_1$) is 11 kcal/mol (8 kcal/mol) by using B3LYP/6–31G*. The gas-phase B3LYP/6–31G* values are close to those obtained by Martí *et al.* (31) from MP2/6–31G* calculations. The results from the SCC-DFTB calculations are in a reasonably good agreement with those from B3LYP/6–31G*, although the energy differences between CHAIR and $DIEQ_2$ or $DIEQ_1$ are somewhat smaller; see Table 1. The large energy difference between CHAIR and $DIEQ_2$ (11.3 kcal/mol with PCM correction) suggests that the population of CHAIR is very small in

Table 1. Energies and structural parameters from calculations

	B3LYP/6-31G*†								SCC-DFTB‡				
Conf§	ΔE	$\Delta\Delta G_{solv}$	R_1	τ_1	τ_2	τ_3	δ	ΔE	R_1	τ_1	τ_2	τ_3	δ
CHAIR	17.9	−6.6	3.8	−132.6	90.5	73.0	20.9	13.8	3.5 (3.3)	−124.0 (−136.0)	101.1 (90.3)	81.2 (65.4)	11.5 (22.9)
$DIEQ_1$	2.9	0.7	4.4	−60.8	169.3	78.8	−54.3	3.5	4.1 (4.0)	−60.9 (−60.2)	168.7 (169.7)	83.3 (78.1)	−53.9 (−54.8)
$DIEQ_2$	0.0	0.0	5.3	−74.9	161.0	−105.8	−43.1	0.0	5.9 (5.3)	−80.0 (−83.0)	154.0 (153.1)	−127.0 (−100.7)	−37.0 (−35.1)
DIAX			4.9¶	−160.2¶	70.9¶	−57.6¶	44.7¶		(4 to 5.5)	(−140 to −180)	(60 to 100)	(−30 to −70)	(15 to 55)
ex-DIAX	12.3	−6.4	5.2	−160.1	70.5	−120.5	44.8						

ΔE and $\Delta\Delta G_{solv}$ values are in kcal/mol. The energies of $DIEQ_2$ are taken as the zero. $R_1 = R(C_1 \ldots C_9)$ (Å), $\tau_1 = \tau(O_7—C_3—C_4—O_{12})$, $\tau_2 = \tau(H—C_3—C_4—H)$, $\tau_3 = \tau(C_8—O_7—C_3—C_2)$, and $\delta = 1/2(|\tau_1| - |\tau_2|)$. Except where otherwise noted, ΔE values and the structural parameters were obtained from the gas-phase calculations. The values of R_1, τ_1, τ_2, τ_3, and δ for the experimental transition-state analogue structure are about 1.53 Å, −149°, 87°, 57°, and 31°, respectively.

†$\Delta\Delta G_{solv}$ values were obtained using the PCM approach. The total gas-phase energies are −837.1571, −837.1810, −837.1857, and −837.1661 a.u. for CHAIR, $DIEQ_1$, $DIEQ_2$, and ex-DIAX, respectively. The solvation free energies are −179.8, −172.5, −173.2, and −178.8 kcal/mol for CHAIR, $DIEQ_1$, $DIEQ_2$, and ex-DIAX, respectively.

‡The structural parameters in parentheses were based on the minimization of chorismate (CHAIR, $DIEQ_1$, and $DIEQ_2$) within a sphere of water molecules or based on molecular dynamics simulations (DIAX).

§See Fig. 2 for definitions.

¶HF/6-31G*; with eight bridging waters (see Fig. 2).

solution, much smaller than the 12% estimated from the NMR measurements of Copley and Knowles (22). As shown in Table 1, one structural difference between CHAIR and DIEQs is that $\tau(O_7—C_3—C_4—O_{12})$ (τ_1) and $\tau(H—C_3—C_4—H)$ (τ_2) are about $-135°$ and 90°, respectively, in CHAIR, whereas they are about $-70°$ and 160°, respectively, in DIEQs. The parameter δ, which is a linear combination of τ_1 and τ_2 (i.e., $\delta = 1/2(\tau_1 - \tau_2)$, is useful for monitoring conformational transitions; i.e., δ is positive for the pseudodiaxial conformers (e.g., CHAIR and DIAX) and negative for the pseudodiequatorial conformers (e.g., $DIEQ_1$ and $DIEQ_2$).

To explore the possible solution conformers, molecular dynamics simulations were performed with the QM/MM method (with or without two guanidinium cations interacting with the two carboxylates) starting from the CHAIR conformer. Although CHAIR is a local minimum in the gas phase, it is not stable in solution. Instead, it is rapidly (within 10–20 ps) converted to another conformer, called DIAX (see Fig. 2), and it spends most of the time in the DIAX conformation during the remainder of the simulations (several hundred picoseconds). Efforts to stabilize CHAIR in solution by the addition of harmonic constraints to the two guanidinium cations at their optimum positions for interaction with the two carboxylates in CHAIR were unsuccessful; CHAIR converted to DIAX by breaking one or more salt-bridge interactions with guanidinium cations. DIAX is not stable by itself in the gas phase, because the two carboxylates are near each other. A stable DIAX conformer was obtained from *ab initio* calculations when water molecules were introduced to bridge the two carboxylates; an optimized DIAX structure from the HF/6–31G* calculations with eight bridging waters is shown in Fig. 2. As can be seen from Fig. 2, there exist structures of the form: CO_2^- . . . HOH. . . O_2^-C- and -CO_2^-. . . $(H_2O)_n$. . . HOH. . . O_2^- C-, where $n = 1$ or 2. Similar structures were found during the QM/MM simulations to stabilize the DIAX conformer in solution; the structural data for the solution conformation are given in Table 1. Such water-bridged structures stabilizing two charged ionic groups have been observed in an earlier simulation of the active site of ribonuclease A (44). Of particular interest about DIAX (see Table 1) is that the dihedral angles describing the ring (τ_1 and τ_2) are similar to those found in CHAIR; DIAX is distinguished from the latter by $\tau_3(C_8—O_7—C_3—C_2)$; i.e., τ_3 is about 70° in CHAIR, whereas it is about $-30°$ to $-70°$ in DIAX, corresponding to the fact that DIAX has the side-chain carboxyl group, rather than the side-chain methylene group, over the C_1 atom. Thus, DIAX is an inactive conformation, but it may well be the one observed by Copley and Knowles (22) in their solution NMR studies; its structure is consistent with the NMR measurement of Hilvert and coworkers (23).

A nonreactive extended pseudodiaxial conformer (ex-DIAX in Fig. 2), which is 5 kcal/mol more stable than CHAIR in the gas phase, was obtained in earlier studies (24–25, 27–28, 31–32). This conformer was identified previously (24, 27), with the pseudodiaxial conformer observed in the NMR studies of Copley and Knowles (22). The structural data for ex-DIAX are also listed in Table 1; most of the parameter values of ex-DIAX are similar to those of DIAX except for τ_3, which is more negative (i.e., $-120°$ instead of $-30°$ to $-70°$ for DIAX), as expected for an extended conformation. Fixed HF/6–31G* structures and Electrostatic Potential Surface charge distributions of ex-DIAX and $DIEQ_2$ were used by Carlson and Jorgensen (27) to study the conformational equilibrium of chorismate in solution. However, ex-DIAX is unstable in solution, and the two carboxylates moved closer to each other and were bridged by water molecules.

The results obtained in this section, in agreement with the experiments of Hilvert and coworkers (23), indicate that the original proposal in which the enzyme preferentially binds the CHAIR conformer is not tenable, because its concentration in solution is too small. Instead, a likely possibility is that DIAX, which could have been mistaken for CHAIR in the original NMR work and is relatively stable in solution, is one of the conformers bound by the enzyme.

Conformation Dynamics in the Active Site of Yeast CM (YCM). The dynamics of CHAIR, $DIEQ_1$, and DIAX were studied in the active site of YCM; $DIEQ_2$ and ex-DIAX were not considered further, because the significant conformational changes required for them to change into CHAIR are unlikely in the active site (10, 11), and the relative positions of the functional groups (i.e., the two carboxylates, the ether oxygen, and the C_4 hydroxyl group) in these (extended) conformations prevent interactions with the corresponding active site residues. As described in *Methods*, energy minimizations were performed first on the complexes with the three different substrate conformers docked in the active site (see Fig. 3). Fig. 3*A* shows that the interactions of CHAIR with the active site residues remain the same as those observed in the x-ray structure (10, 11). As a result of the minimization, the interaction distances are improved significantly from the values in the docked structure (see Fig. 3*A* legend). The R_1 distance is 2.9 Å, about 0.5 Å smaller than that obtained in the gas phase (3.5 Å) and in solution (3.3 Å). Fig. 3*B* shows that $DIEQ_1$ retains its conformation after the minimization (i.e., it has essentially the same structure as that shown in Fig. 2). Almost all of the electrostatic and hydrogen-bonding interactions between YCM and CHAIR in the YCM–CHAIR complex discussed above are found in the YCM–$DIEQ_1$ complex, including the one involving the backbone amide group of Asn-194 and the C_4 hydroxyl oxygen missing in the initial docked structure (see *Methods*); the only exception is that the hydroxyl hydrogen of C_4 still makes the internal hydrogen bond with the side-chain carboxylate. Fig. 3*C* shows that, whereas energy minimization moves DIAX somewhat closer to CHAIR (i.e., $R_1 = 3.6$ Å and $\tau_3 = 2°$ compared with $R_1 = 4–5$ Å and $\tau_3 = -30°$ to $-70°$ of DIAX in solution; in CHAIR, the values are $R_1 = 3.3$ Å and $\tau_3 = 65°$), the environment of the ring carboxylate is different from that observed in the TSA x-ray structure (10–11). Specifically, Arg-157 interacts only with one of the ring carboxylate oxygens in DIAX (it interacts with both ring carboxylate oxygens in CHAIR), and the hydroxyl proton of Thr-242 is 6.7 Å away from O_b (the distance for CHAIR is 1.7 Å). Moreover, the C_4 hydroxyl of DIAX cannot hydrogen bond to Glu-198 and the backbone amide group of Asn-194 at the same time, in contrast to the CHAIR. These differences result from the incorrect orientation of the side chain with respect to the ring in DIAX, even after minimization. The minimized structures shown in Fig. 3 *B* and *C* for $DIEQ_1$ and DIAX, respectively, are not appropriate for the Claisen rearrangement, and catalysis starting with them would require large structural changes during the reaction.

To determine whether the reorientation of DIAX and $DIEQ_1$ is likely to occur spontaneously and rapidly before reaction, we did QM/MM molecular dynamics simulations in the active site. The motions of CHAIR, $DIEQ_1$, and DIAX in the enzyme active site are monitored in Fig. 4 by using τ_3 and/or the angle δ. Fig. 4*A* (*Top*) shows that, in contrast to the motion of CHAIR in solution (see above), no conformational transition occurs in the active site; the substrate remains in the neighborhood of CHAIR, with δ about 30° and τ_3 about 60°; the values for the minimized CHAIR are 25° and 59°, respectively (see caption to Fig. 3*A*). Moreover, the important interactions with the active site residues shown in Fig. 3*A* are retained. The conformational changes of $DIEQ_1$ at 100 and 200 K are monitored by δ in Fig. 4*B* (*Middle*); the behavior at 300 K is similar to that at 200 K. The δ value for $DIEQ_1$ is about $-45°$ for the substrate within the enzyme after energy minimization ($\approx$-55° in the gas phase or minimized in solution), whereas it is about 12–23° for CHAIR

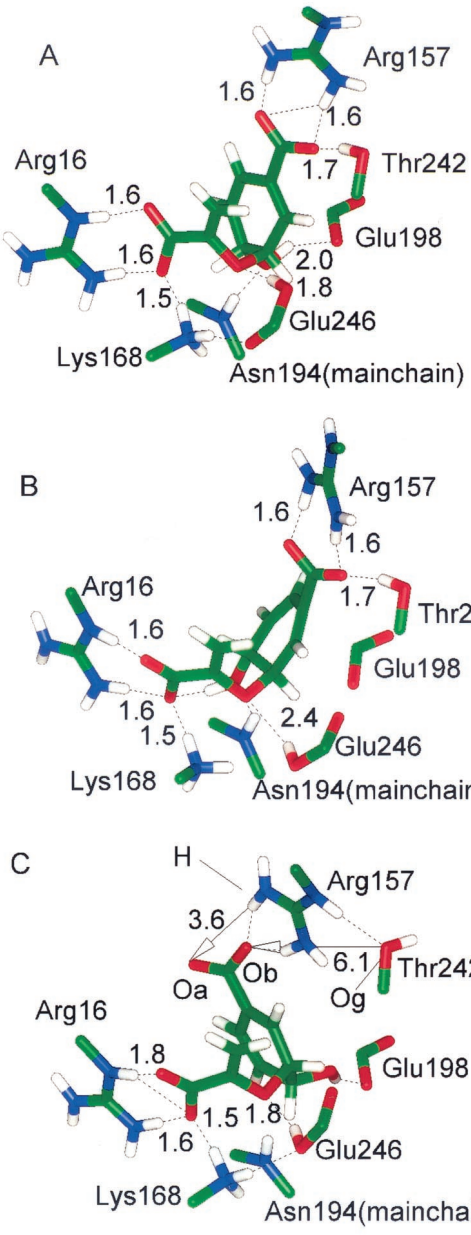

Fig. 3. Active site structures after energy minimization and before dynamics. (*A*) CHAIR. The interactions between the substrate and the active site residues are the same as those observed in the x-ray structures (10–11). The interactions and distances are (with the values in the initial docked structure given in parentheses): 1) salt bridge between Arg-16 and the side-chain carboxylate with the corresponding distances between the protons of Arg-16 and the oxygens equal to 1.6 Å (2.0–2.3 Å); 2) salt bridge between Lys-168 and the side-chain carboxylate with a distance between the proton of Lys-168 and the oxygen of the carboxylate equal to 1.5 Å (2.5 Å); 3) salt bridge between Arg-157 (H) and the ring carboxylate (O) with distances equal to 1.6 Å (1.9–2.5 Å); 4) hydrogen bond between Glu-246 (H) and the ether oxygen with a distance equal to 1.8 Å (2.3 Å); 5) hydrogen bond between Lys-168 (H) and the ether oxygen with a distance equal to 2.4 Å (2.6 Å); 6) interaction between Thr-242 (H) and the ring carboxylate with a distance equal to 1.7 Å (2.9 Å); 7) interaction between the backbone amide group (H) of Asn-194 and the hydroxyl oxygen with a distance equal to 1.9 Å (2.7 Å); and 8) interaction between Glu-198 and the C_4 hydroxyl proton with a distance equal to 2.0 Å (3.5 Å). The energy minimization of the YCM–CHAIR complex does not lead to a different conformation, although there are some modifications of the structural parameters (see above). $R_1 = 2.9$ Å, $\tau_1 = -137°$, $\tau_2 = 87°$, $\tau_3 = 59°$, and $\delta = 25°$. (*B*) $DIEQ_1$. The substrate is still in $DIEQ_1$ after the energy minimization. $R_1 = 3.7$ Å, $\tau_1 = -70°$, $\tau_2 = 160°$, $\tau_3 = 68°$, and $\delta = -45°$. All of the interactions in *A* exist here, except that the hydroxyl proton is involved in the internal hydrogen bond with the side-chain carboxylate rather than with Glu-198 (8 above). (*C*) DIAX. The initial orientation of DIAX in the active site is such that the side-chain groups (the carboxylate and ether oxygen) form the observed interactions with the active residues (i.e., 1, 2, 4, and 5). The substrate undergoes a rotation about the C_3—O_7 bond (R_2) toward CHAIR during the minimization, so the conformation is between DIAX and CHAIR. $R_1 = 3.6$ Å, $\tau_1 = -145°$, $\tau_2 = 84°$, $\tau_3 = 2°$, and $\delta = 31°$. Certain interactions involving the ring carboxylate and the C_4 hydroxyl proton cannot be formed; e.g., Arg-157 interacts only with one of the ring carboxylate oxygens, and the hydroxyl group of Thr-242 is 6 Å away from the oxygen (O_b) of the ring carboxylate.

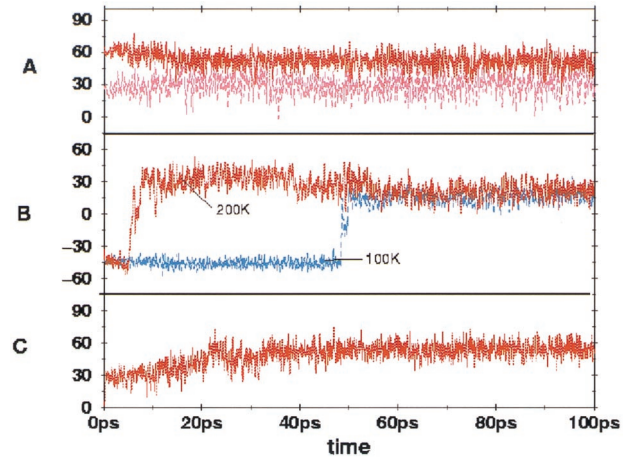

Fig. 4. Motions of CHAIR, $DIEQ_1$, and DIAX in the active site of YCM as a function of time. (*A*) CHAIR at 300 K. The motion is monitored by δ (magenta, dashed line) and τ_3 (red, dotted line). No conformational transition occurs, and the substrate remains in the neighborhood of CHAIR (i.e., $\delta \approx 30°$ and $\tau_3 \approx 60°$). (*B*) $DIEQ_1$ at 100 K (blue, dashed line) and 200 K (red, dotted line). The motion is monitored by δ. The substrate changes to CHAIR in about 50 ps at 100 K and 5–10 ps at 200 K, as indicated by the change of δ from negative to positive values. (*C*) DIAX at 300 K. The motion is monitored by τ_3 (red, dotted line). τ_3 increases from 0° to 50–60° (CHAIR) as a result of the rotation of the ring carboxylate.

(see Table 1). Fig. 4*B* (*Middle*) shows that the substrate changes to CHAIR with δ in the range of 5–40° in about 50 ps at 100 K and 5–10 ps at 200 K (or 300 K). It then fluctuates around the CHAIR conformation during the remainder of the simulation time (500 ps). The fluctuations after the transition are larger than those before, in part because of the absence of the internal hydrogen bond between the C_4 hydroxyl proton and the side-chain carboxylate. Fig. 5*A* examines the internal hydrogen bond between the C_4 hydroxyl proton and side-chain carboxylate in $DIEQ_1$ at 100 and 200 K as a function of time. It is evident that this hydrogen bond is broken at the same time as the substrate changes from $DIEQ_1$ to CHAIR (see Fig. 4*B*). As mentioned earlier, the only interaction between the substrate and active site residues that is lacking in the YCM–$DIEQ_1$ complex, relative to those in the YCM–CHAIR complex, is the hydrogen bond between the C_4 hydroxyl proton and Glu-198, as long as the hydroxyl proton is involved in the internal hydrogen bond.

The simulation of DIAX at 300 K (Fig. 4*C*, *Bottom*) shows that τ_3, the torsional angle reflecting the relative orientation of the side chain and ring, initially moves from about 0° (the value after the minimization) to 30° in about 1 ps and then gradually increases to 50–60° by 50 ps, when the transition to CHAIR is essentially complete; the δ value is not sensitive to the transition, as it is similar in the pseudodiaxial conformers DIAX and CHAIR (i.e., 10–40°; see Table 1 and the discussions above). Fig. 5*B* shows the time dependence for the YCM–DIAX complex of the interactions that exist in the YCM–CHAIR complex

BIOCHEMISTRY

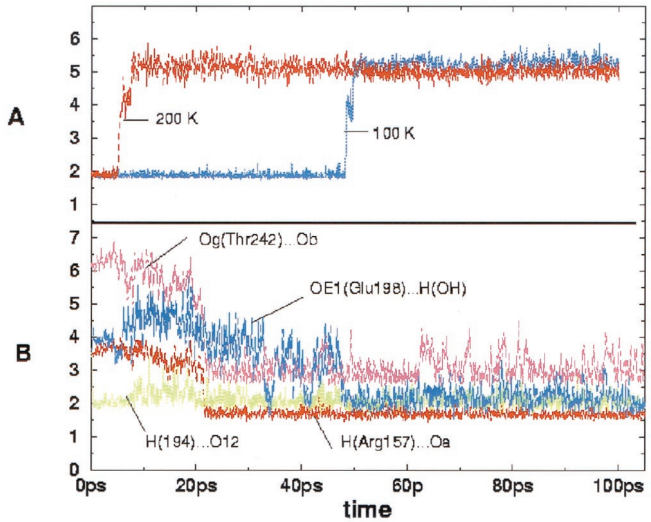

Fig. 5. (*A*) The internal hydrogen bond between the C_4 hydroxyl proton and the side-chain carboxylate oxygen in the YCM–$DIEQ_1$ complex monitored as a function of time; the trajectories shown are the ones used to produce Fig. 4*B*. This figure shows that the hydrogen bond is broken at the same time as the conformation transition from $DIEQ_1$ to CHAIR occurs at each temperature (compare Fig. 4*B*). (*B*) Certain interactions of the ring carboxylate and C_4 hydroxyl group with the active site residues (Arg-157, Thr-242, Glu-198, and Asn-194) in the YCM–DIAX complex as functions of time. The trajectory is the one used to produce Fig. 4*C*. There are no interactions initially between H of Arg-157 and O_a of the ring carboxylate, between Thr-242 and O_b, and between O_{E1} of Glu-198 and the C_4 hydroxyl proton in the YCM–DIAX complex (see Fig. 3*C*). *B* shows that these interactions are all formed after 50-ps simulations as the substrate changes from DIAX to CHAIR.

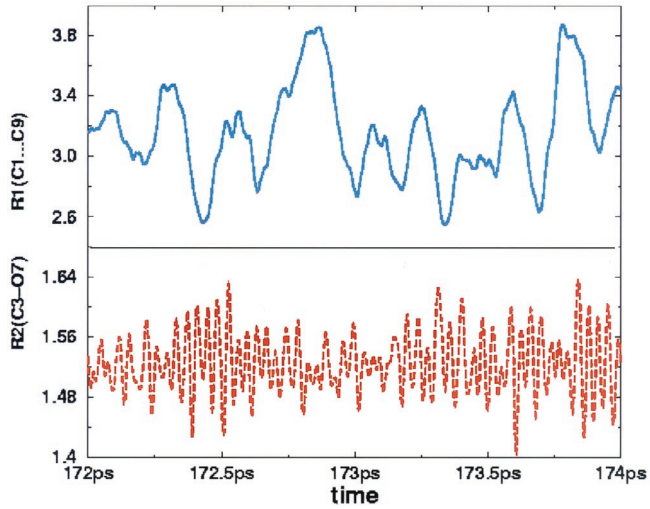

Fig. 6. The fluctuations of the $C_1 \ldots C_9$ distance (R_1) and the C_3—O_7 distance (R_2) during 2 ps (from 172 to 174 ps) in the active site at 300 K, starting from the minimized structure in Fig. 3*A*. R_1, blue-solid line; R_2, red-dashed line.

but are absent initially in the YCM–DIAX complex. The distances examined are between the hydroxyl group (O_g) of Thr-242 and O_b of the ring carboxylate, between H of Arg-157 (see Fig. 3 for the designation) and O_a of the ring carboxylate, and between O_{E1} of Glu-198 and the C_4 hydroxyl proton of the substrate; the hydrogen bond distance between the main-chain amide group of Asn-194 and the C_4 hydroxyl oxygen is also monitored. Fig. 5*B* shows that all these interactions are formed after 50 ps, consistent with the transformation to a CHAIR-like structure (Fig. 4*C*). We note that the side-chain carboxylate is anchored by its interactions with Arg-16, Lys-168, and Glu-246 (Lys-168 and Glu-246 are held together by a strong hydrogen bond) so that it is the ring that rotates to achieve the CHAIR conformation of lower energy. Glu-246 is near the ether oxygen in the x-ray YCM-TSA structure, and a previous simulation (33) shows that it is protonated and hydrogen bonded to the ether oxygen.

The fluctuations of the $C_1 \ldots C_9$ distance (R_1) and the C_3—O_7 bond (R_2) of CHAIR in the active site at 300 K are monitored in Fig. 6; the data were obtained from the same trajectory that produced Fig. 4*A*. The fluctuations over 2 ps (172–174 ps) are shown; corresponding behavior is observed in the rest of the trajectory. The distance between C_1 and C_9, which form a covalent bond during the reaction, can be as short as 2.5 Å. Moreover, there are numerous instances during the dynamics where R_1 decreases from its equilibrium distance (2.9 Å at the active site), whereas R_2 increases slightly. These transient structures are closer to the transition state than the stable CHAIR conformer.

Discussion

Experiments by Knowles and coworkers (refs. 18 and 19) have shown that the rearrangement of chorismate to prephenate proceeds through a chair-like transition state both in solution and in the enzyme. This result has led to the suggestion that the reaction starts from the chair, pseudodiaxial conformer (CHAIR) where C_1 and C_9 are positioned to form a carbon—carbon bond. Thus, one way for CM to catalyze the reaction is to bind the CHAIR conformer preferentially from solution and to catalyze its chemical transformation at the active site. A requirement for this mechanism is a sufficiently large population of CHAIR in solution.

Copley and Knowles (22) measured the temperature variation of the ^1H coupling constants for the protons in the ring of chorismate and showed that, whereas the pseudodiequatorial conformation(s) is dominant, a pseudodiaxial conformer(s) exists at reasonable levels (≈12%) in water. They assumed it was the CHAIR conformer, but the results of the present solution simulations suggest that the NMR data are likely to correspond to a nonchair, pseudodiaxial conformer (DIAX), which has the side-chain carboxylate group instead of the methylene group over the C_1 atom (the $C_1 \ldots C_9$ distance is 5 Å) and so is in an inactive conformation. Indeed, the CHAIR conformer is unstable in solution, and the solution simulations starting from CHAIR lead to the stable DIAX in 10–20 ps. DIAX may not be distinguishable from CHAIR, on the basis of the coupling constants of the ring protons. Moreover, the study of the transferred nuclear Overhauser effects for chorismate in solution (23) showed no evidence for the existence of the CHAIR conformer.

Thus, the enzyme could bind the more abundant nonchair conformations from solution. To determine whether the conversion of such conformers to CHAIR is possible in the enzyme–substrate complex, we have explored the dynamics of DIAX, which is abundant in solution, and a second conformer, $DIEQ_1$, after they are bound to the enzyme in the inactive (solution) conformations. In the active site, both DIAX and $DIEQ_1$ are rapidly converted (within 50 ps at 300 K) to CHAIR in a molecular dynamics simulation using a QM/MM potential for the enzyme–substrate complexes. This result suggests that the selection of the reactive CHAIR conformer is *not* necessary for the CM-catalyzed reaction. Instead, more abundant conformers can be bound and converted to the active CHAIR form in a fast step that is not rate limiting.

A recent transferred nuclear Overhauser effect study of the catalytic antibody 1F7 (23) indicates that, whereas the CHAIR conformer is not observed in solution, it is detectable in the

antibody 1F7: the preorganization apparently takes place at the antibody active site. The present study suggests that this may well be true for the CM from yeast and perhaps for CM from other species. Because the conformational transformations from nonreactive conformers to the reactive CHAIR are very efficient in the natural enzyme, they could play a role in the catalytic mechanism.

Dynamics of the CHAIR form in the active site result in structures that approach the transition state for the length of the bond to be formed and the orientation of the methylene group. This result is in part a consequence of the use of a QM/MM potential, which would lead to reaction in the simulations if the barrier were low enough. The relation of this observation to catalysis is of interest (45).

Helpful discussions with Dr. Jianpeng Ma are gratefully acknowledged. This work was supported by Grant GM06920 (W.N.L.) from the National Institutes of Health and by grants (M.K.) from the Department of Energy and the National Institutes of Health. Parts of the computations were done on the J90 at National Energy Research Scientific Computing and the SGI Origin 2000 at National Center for Supercomputing Applications.

1. Lee, A. Y., Clardy, J., Stewart, J. D. & Ganem, B. (1995) *Chem. Biol.* **2,** 195–203.
2. Braus, G. H. (1991) *Microbiol. Rev.* **55,** 349–370.
3. Andrews, P. R., Smith, G. D. & Young, I. G. (1973) *Biochemistry* **12,** 3492–3498.
4. Bartlett, P. A. & Johnson, C. R. (1985) *J. Am. Chem. Soc.* **107,** 7792–7793.
5. Gorisch, H. (1978) *Biochemistry* **18,** 3700–3705.
6. Kast, P., Asif-Ullah, M. & Hilvert, D. (1996) *Tetrahedron Lett.* **37,** 2691–2694.
7. Hilvert, D., Carpenter, S. H., Nared, K. D. & Auditor, M.-T. M. (1988) *Proc. Natl. Acad. Sci. USA* **85,** 4953–4955.
8. Chook, Y. M., Ke, H. & Lipscomb, W. N. (1993) *Proc. Natl. Acad. Sci. USA* **90,** 8600–8603.
9. Chook, Y. M., Gray, J. V., Ke, H. & Lipscomb, W. N. (1994) *J. Mol. Biol.* **240,** 476–500.
10. Lee, A. Y., Karplus, P. A., Ganem, B. & Clardy, J. (1995) *J. Am. Chem. Soc.* **117,** 3627–3628.
11. Strater, N., Schnappauf, G., Braus, G. & Lipscomb, W. N. (1997) *Structure (London)* **5,** 1437–1452.
12. Haynes, M. R., Stura, E. A., Hilvert, D. & Wilson, I. A. (1994) *Science* **263,** 646–652.
13. Cload, S. T., Liu, D. R., Pastor, R. M. & Schultz, P. G. (1996) *J. Am. Chem. Soc.* **118,** 1787–1788.
14. Liu, D. R., Cload, S. T., Pastor, R. M. & Schultz, P. G. (1996) *J. Am. Chem. Soc.* **118,** 1789–1790.
15. Kast, P., Hartgerink, J. D., Asif-Ullah, M. & Hilvert, D. (1996) *J. Am. Chem. Soc.* **118,** 3069–3070.
16. Kast, P., Asif-Ullah, M., Jiang, N. & Hilvert, D. (1996) *Proc. Natl. Acad. Sci. USA* **93,** 5043–5048.
17. Schnappauf, G., Strater, N., Lipscomb, W. N. & Braus, G. (1997) *Proc. Natl. Acad. Sci. USA* **94,** 8491–8496.
18. Sogo, S. G., Widlanski, T. S., Hoare, J. H., Grimshaw, C. E., Berchtold, G. A. & Knowles, J. R. (1984) *J. Am. Chem. Soc.* **106,** 2701–2703.
19. Copley, S. D. & Knowles, J. R. (1985) *J. Am. Chem. Soc.* **107,** 5306–5308.
20. Gray, J. V., Eren, D. & Knowles, J. R. (1990) *Biochemistry* **29,** 8872–8878.
21. Guilford, W. J., Copley, S. D. & Knowles, J. R. (1987) *J. Am. Chem. Soc.* **109,** 5013–5019.
22. Copley, S. D. & Knowles, J. R. (1987) *J. Am. Chem. Soc.* **109,** 5008–5013.
23. Campbell, A. P., Tarasow, T. M., Massefski, W., Wright, P. E. & Hilvert, D. (1993) *Proc. Natl. Acad. Sci. USA* **90,** 8663–8667.
24. Wiest, O. & Houk, K. N. (1995) *J. Am. Chem. Soc.* **117,** 11628–11639.
25. Khanjin, N. A., Snyder, J. P. & Menger, F. M. (1999) *J. Am. Chem. Soc.* **121,** 11831–11846.
26. Gustin, D. J., Mattei, P., Kast, P., Wiest, O., Lee, L., Cleland, W. W. & Hilvert, D. (1999) *J. Am. Chem. Soc.* **121,** 1756–1757.
27. Carlson, H. A. & Jorgensen, W. L. (1996) *J. Am. Chem. Soc.* **118,** 8475–8484.
28. Lyne, P. D., Mulholland, A. J. & Richards, W. G. (1995) *J. Am. Chem. Soc.* **117,** 11345–11350.
29. Davidson, M. M., Gould, I. R. & Hillier, I. H. (1995) *J. Chem. Soc. Chem. Commun.* 63–64.
30. Davidson, M. M., Gould, I. R. & Hillier, I. H. (1996) *J. Chem. Soc. Perkins Trans. 2*, 525–532.
31. Martí, S., Andrés, J., Moliner, V., Silla, E., Tuñón, I. & Bertrán, J. (2000) *J. Phys. Chem. B* **104,** 11308–11315.
32. Martí, S., Andrés, J., Moliner, V. Silla, E., Tuñón, I., Bertrán, J. & Field, M. J. (2001) *J. Am. Chem. Soc.* **123,** 1709–1712.
33. Ma, J., Zheng, X., Schnappauf, G., Braus, G., Karplus, M. & Lipscomb, W. N. (1998) *Proc. Natl. Acad. Sci. USA* **95,** 14640–14645.
34. Cui, Q., Elstner, M., Kaxiras, E., Frauenheim, T. & Karplus, M. (2001) *J. Phys. Chem. B* **105,** 569–585.
35. Elstner, M., Porezag, D., Jungnickel, G., Elsner, J., Haugk, M., Frauenheim, T., Suhai, S. & Seifert, G. (1998) *Phys. Rev. B* **58,** 7260–7268.
36. Frisch, M. J., Trucks, G. W., Schlegel, H. B., Scuseria, G. E., Robb, M. A., Cheeseman, J. R., Zakrzewski, V. G., Montgomery, J. A., Jr., Stratmann, R. E., Burant, J. C., *et al.* (1998) GAUSSIAN98 (Gaussian, Pittsburgh, PA).
37. Cossi, M., Barone, V., Cammi, R. & Tomasi, J. (1996) *Chem. Phys. Lett.* **255,** 327–335.
38. Brooks, B. R., Bruccoleri, R. E., Olafson, B. D., States, D. J., Swaminathan, S. & Karplus, M. (1983) *J. Comput. Chem.* **4,** 187–217.
39. MacKerell, A. D., Jr., Bashford, D., Bellott, M., Dunbrack, R. L., Jr., Evanseck, J. D., Field, M. J., Fischer, S., Gao, J., Guo, H., Ha, S., *et al.* (1998) *J. Phys. Chem., Ser. B* **102,** 3586–3616.
40. Jorgensen, W. L. (1981) *J. Am. Chem. Soc.* **103,** 335–340.
41. Neria, E., Fisher, S. & Karplus, M. (1996) *J. Chem. Phys.* **105,** 1902–1921.
42. Brooks, C. L., III, Brunger, A. & Karplus, M. (1985) *Biopolymers* **24,** 843–865.
43. Brunger, A., Brooks, C. L., III, & Karplus, M. (1985) *Proc. Natl. Acad. Sci. USA* **82,** 8458–8462.
44. Bruice, T. & Benkovic, S. J. (2000) *Biochemistry* **39,** 6267–6274.